Highlights of Spanish Astrophysics XI, Proceedings of the XV Scientific Meeting of the Spanish Astronomical Society held on September 4–9, 2022, in La Laguna, Spain. M. Manteiga, L. Bellot, P. Benavidez, A. de Lorenzo-Cáceres, M. A. Fuente, M. J. Martínez, M. Vázquez- Acosta, C. Dafonte (eds.), 2023

Continuum and line emission of the symbiotic binary R Aqr.

Gómez-Garrido, M.[1], Bujarrabal, V [2], Alcolea, J.[1], and Castro-Carrizo, A.[3]

[1] Observatorio Astronómico Nacional (OAN-IGN), C/ Alfonso XII, 3, 28014 Madrid, Spain
[2] Observatorio Astronómico Nacional (OAN-IGN), Apartado 112, 28803 Alcalá de Henares, Spain
[3] Institut de Radioastronomie Millimétrique, 300 rue de Piscine, 38406 Saint Martin d'Hères, France

Abstract

Symbiotic stellar systems (SSs) are interacting binaries consisting of two close components: an asymptotic giant branch (AGB) star and a white dwarf (WD). As a result of the mass loss of the AGB star, SSs are surrounded by a circumstellar environment whose shape and dynamics are affected by the presence of the hot companion. The study of SSs is key to understanding different phenomena, such as jets, non-spherical planetary nebulae, and Type Ia supernovae. R Aqr is one of the best-studied SSs. The orbit shows a period of ~ 42 years with a stellar separation between 10 and 60 mas. Although R Aqr shows molecular emission in some species, due to the photodissociation by the WD, this is rarely detected in SSs. We present high- and medium-resolution ALMA observations of the continuum and line emission exploring both extended and inner regions of this SS system for a total of three ALMA bands (6, 7, and 9). Continuum emission helps to locate the position of the AGB in the system. In addition, the jets and the mass transfer from the AGB to the WD are mapped by the continuum. Some of the studied lines are CO, SiO, SO, and $H30_{\alpha}$. We describe a new scenario for the molecular emission in R Aqr explaining the brightness distributions shown by the different lines.

1 Introduction

Symbiotic stellar systems (SSs) are interacting binaries composed by an evolved star and a compact object. In the particular case of the D-type symbiotics, which show intense continuum dust emission, the systems are formed by two close components: the primary, an asymptotic giant branch (AGB) and the secondary, a white dwarf (WD) [5]. The material ejected by the AGB component falls to the WD forming an accretion disk around the secondary component. The jets observed in SSs emerge from the central region of these accretion disks. The study of the symbiotic binaries can be a fundamental to understanding the morphology found in planetary nebulae. By observing, modeling, and studying the molecular gas and dust in these objects, we can learn more about the non-spherical structures that appear in the final stage of Sun-like stars.

Due to the intense ultraviolet (UV) emission from the hot component, most of the molecules are photodissociated. As a result, only CO, SiO and H_2O are detected in some SSs, such as R Aqr and CH Cyg [1]. R Aqr is the best-studied symbiotic stellar system. The inner region of the nebula is dominated by a precessing jet (see [9] and [4]). The primary component of this system is a Mira-type

variable with a pulsation period of 388 days, and the secondary is a white dwarf. A size of 15 mas for the primary component is estimated from measurements of R Aqr in the Infrared range [7]. The distance to R Aqr from Gaia parallax is 320 pc, while the distance derived from VLBI observation of SiO masers is 218 pc [6]. The origin of this difference is unknown, but these discrepancies are also found in distances calculated from Gaia parallaxes for other objects with nebulous structures. We assume an intermediate value for the distance adopting 265 pc in our calculations. New orbital parameters have been derived recently (see the contribution by Alcolea *et al.* in these proceedings). The white dwarf describes an elliptical orbit with a period of 42.4 yr. The major semi-axis is 57 mas with an inclination angle of 110 deg, which means that the white dwarf is moving almost in the right ascension (R.A) direction. We have studied the molecular line and continuum emissions of R Aqr and the spatial distribution of the material in this symbiotic system.

2 ALMA observations

We observed R Aqr using the Atacama Large Millimeter/sub-millimeter Array (ALMA). We have used three ALMA bands, namely 6, 7, and 9, corresponding to 1.3, 0.9, and 0.45 mm, and angular resolutions between 20 and 250 mas. Thanks to the high spatial resolution provided by the extended ALMA configurations, we can probe the inner region of R Aqr. The observations of Band 6 were carried out using the extended and compact configuration of ALMA. In this case, both data sets are mixed to achieve a higher signal-to-noise ratio (S/N). To study the main molecular lines, such as CO and SiO, in detail, high spectral units of the correlator were connected. Moderate spectral resolution units were also used simultaneously to derive the continuum emission with good S/N.

The position of both components of R Aqr varies in time because of proper motion and their orbital movements. Since the observations at the different frequencies were performed on different dates, we center all our *uv*-tables to the centroid of the continuum emission at each frequency to present our data in the same reference framework. As a result, our final maps are expected to be referenced to the AGB position for all observations.

Note that to better study the line emission, the continuum distribution was subtracted and it can affect the brightness distribution observed in the line maps in a complex way. We also study the continuum emission of R Aqr. Since the high- and low-resolution continuum maps at 0.9 mm were studied by [2] in detail, we focus on the analysis of the observation at 1.3 and 0.45 mm.

3 Continuum and H30α maps

Fig. 1(a) shows the low spatial resolution image of the continuum emission of R Aqr at 1.3 mm, where we can see the large-scale emission of the jet. Fig. 1(b) shows the high resolution continuum maps at 1.3 and 0.45 mm, bands 6 and 9 respectively. The high-resolution maps let us study the inner region of R Aqr where the formation of the jet is taking place. In Fig. 1(b) we can see the emergence of the jet, which connects to the large-scale jet shown by Fig. 1(a). We can also see how the continuum emission at 1.3 mm extends from the central position, where is located the Mira component, to the position of the white dwarf. This suggests a physical connection between both components as previously seen in the continuum data at 0.9 mm (see [2]). However, the angular resolution is not enough to separate the

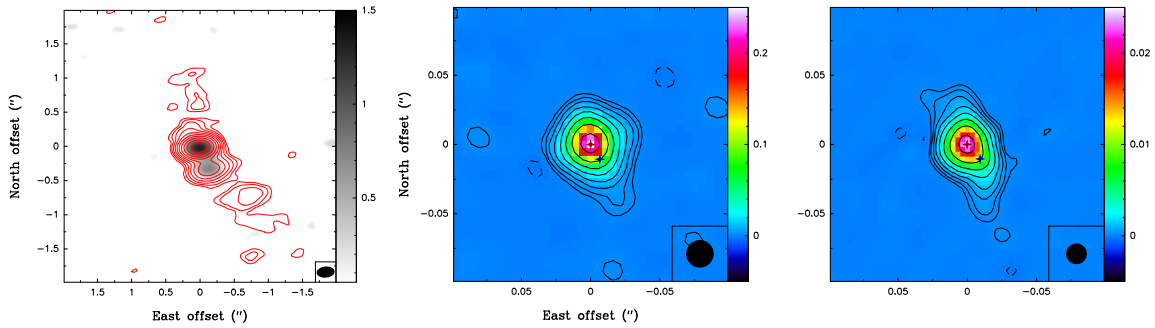

(a) (b)

Figure 1: (*a*): Red contours: low-resolution map of continuum at 1.3 mm towards R Aqr. The contour level spacing is logarithmic with a jump of factor 2. The first positive contour is 0.07 mJybeam^{-1}. The brightness distribution of H30α integrated over all velocities is shown in greyscale. In the inset we can see the beam, with a size of 264×163 mas and P.A. of 95 deg. (*b*):High-resolution continuum maps at 1.3 and 0.45 mm towards R Aqr. The contour level spacing is logarithmic, with a jump of factor two. The first positive contours are 0.15 and 1.5 mJybeam^{-1} respectively. The observations are centered on the continuum centroid, the position of the Mira component (red cross); the predicted position for the WD is also indicated (blue cross). See the beams in the insets, with a size of 15×15 and 20×20 mas respectively.

emission of the radio photo-sphere, jet, and other components. We also studied the emission of H30α. Fig. 1(a) shows the low-resolution emission of this recombination line, which extends in the direction nort-east to south-west. Note that the brightness distribution corresponds to the intensity integrated over the complete velocity range. We find that the distribution of H30α and the continuum show similar structures. This was also found in the Hα in the visual spectral region by [8]. The differences between the continuum and H30α can be caused by the lower sensitivity of the recombination line map. We can estimate the spectral index of the compact component, although this value is highly uncertain due to the intense flux variability of the AGB in time. We obtain a value of 2.2, which is compatible with the emission of dust emitting as a black body. The extended component in Fig. 1(b) is more difficult to understand because in that region the emission of the jet, white dwarf and material falling to the hot companion are all mixed up.

4 Molecular line maps

Many molecular species, such as CO, SiO, SO, and H_2O are detected in R Aqr. Figs. 2 and 3 show the emission of ^{12}CO J=2–1 and ^{28}SiO v=0 J=16–15 as an example of the molecular emission found in this SS. The emission of CO is the most intense and extended. We find a typical size for the emission of CO of 800×200 mas. This means that the CO molecules survive at distances larger than the orbital size. The emission of CO was modeled using hydrodynamical calculations (see [3]). This model predicts the spiral structures around this binary system as a result of the interaction between

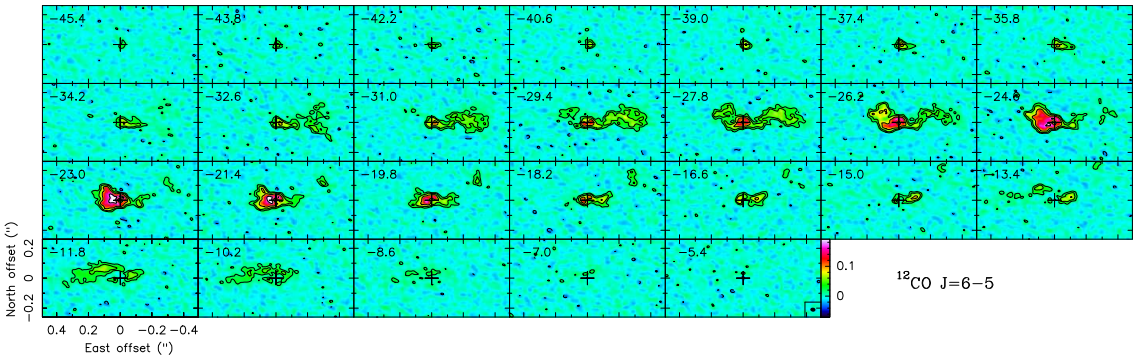

Figure 2: ALMA maps per velocity channel of ^{12}CO J=6–5 emission in R Aqr. Local standard of rest (LSR) velocities are indicated in the upper left corners. The contours are logarithmic, with a jump of factor two and a first level of 2 mJybeam^{-1}. The dashed contours represent negative values. The beam is shown in the inset in the last panel.

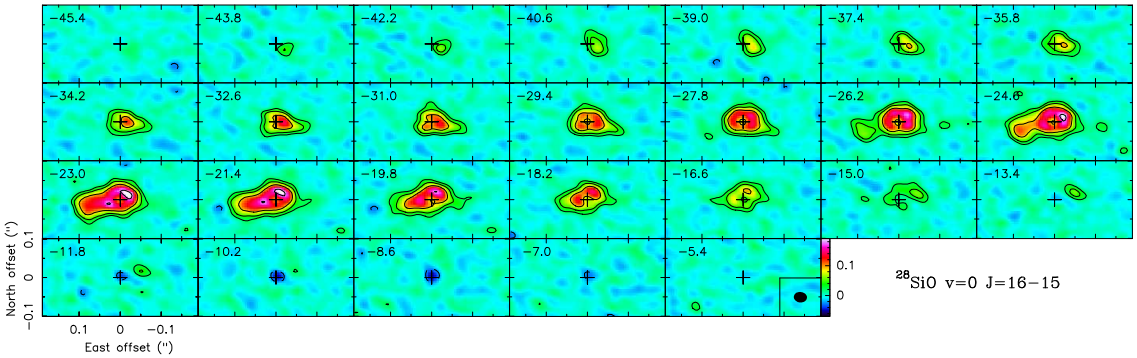

Figure 3: Same as Fig. 2 but for ^{28}SiO v=0 J=16–15 using a first level of 2 mJybeam^{-1}.

the two stellar components.

The SiO molecule shows emission beyond the orbital size in the R.A. direction, but it is not more extended than CO. Note that its extent to the south-east is similar to that seen in CO (see Fig. 4), and therefore, the emissions of both molecules probably come from the same region. We find absorption at positive velocities in many rotational transitions of this molecule and its isotopic substitution ^{29}SiO. We identify this absorption with falling material ejected previously by the AGB component. Note that the extended component of the SiO and CO tends to be confined in the orbital plane, which is in the R.A. direction approximately. We suppose that the molecules out of this region are photodissociated by the UV radiation from the WD.

In the cases of the less abundant molecules, the emission is also more compact. Fig. 4 shows the central velocities maps of several molecular species, which are representative of the shapes shown by the different molecular lines: ^{12}CO J=6–5, ^{28}SiO v=0 J=16–15, SO $^3\Sigma$ v=0 16_{16}–15_{15}, H_2O v_3=1 $5_{7,2}$–$6_{6,1}$, and SiO v=9 J=17–16. Note that the brightness distributions of CO and SiO show a ring-like structure in the central region, while for the less abundant molecules we can distinguish several shapes of brightness distributions: ”peanut”-like, compact and compact-offset. The brightness

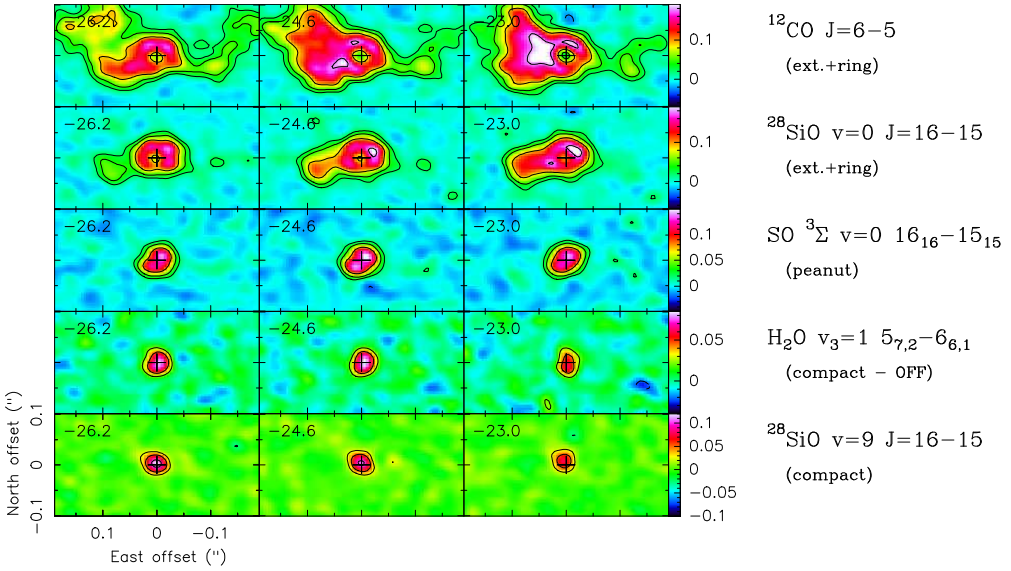

Figure 4: Same as Fig. 2 but for the central velocities ALMA maps of the ^{12}CO J=6–5, ^{28}SiO v=0 J=16–15, SO $^3\Sigma$ v=0, 16_{16}–15_{15}, H_2O v_3=1 $5_{7,2}$–$6_{6,1}$, and SiO v=9 J=17–16 lines.

distributions of the less abundant molecules are more compact, showing emission only in the central region, and in many cases, only inside the orbital region. This behavior means that is very difficult to find little abundant molecules at large distances from the AGB envelope where they are formed. These molecules are photo-dissociated by the WD and only survive in the densest and best-shielded regions close to the AGB.

Gravitational interactions between the WD and the material ejected by the AGB result in a complex dynamical scenario. Therefore, modeling the extended emission shown by the most abundant molecules is very hard. We focus on modeling the compact emission seen in the central region. We model the emission of the ^{28}SiO v=0 J=16–15 line, which is taken as reference, using a radiative transfer model. For the calculations, we take into account two different components: a relatively hot expanding envelope and cool layers falling back onto to the AGB. The resulting map is shown in Fig. 5. We obtain similar theoretical brightness distribution and intensities than the observed per velocity channel for the ^{28}SiO v=0 J=16–15 line. Thanks to the introduction of the falling material we also obtain good results for the absorption feature seen on the positive velocities.

The variety of brightness distribution shown by the different lines can be partially explained by the continuum subtraction. This effect is more important in optically thick molecules, such as CO and SiO, which show a well defined hole in the maps of their central velocity channels. For optically thiner molecules, such as SO and H_2O, the subtraction of the continuum distribution is less noticeable in the final maps.

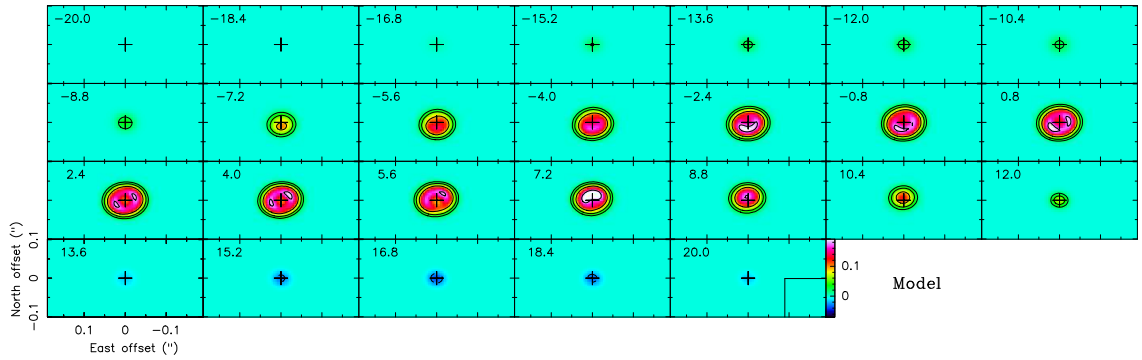

Figure 5: Same as Fig. 2 but for synthetic maps per velocity channel and using a first level of 3 mJybeam^{-1}.

Acknowledgments

Authors acknowledge the support of the Spanish Ministry of Science and Innovation through the Agencia Estatal de Investigación research grant PID2019-105203GB-C21 (EVENTs / Nebulae Web project).

References

[1] Bujarrabal, V., Mikołajewska, J., Alcolea, J., and Quintana-Lacaci, G. 2010, A&A, 516A, 19B

[2] Bujarrabal, V., Alcolea, J., Mikołajewska, J., *et al.* 2018, A&A, 616, L3

[3] Bujarrabal, V., Agúndez, M., Gómez-Garrido, M., *et al.* 2021, A&A 651, A4

[4] Melnikov, S., Stute, M., & Eislöffel, J. 2018, A&A, 612, A77

[5] Mikołajewska, J. 2012, Balt. Astron. 21, 5

[6] Min, C., Matsumoto, N., Kim, M. K., *et al.* 2014, PASJ, 66, 38

[7] Ragland, S., Le Coroller, H., Pluzhnik, E., *et al.* 2008, ApJ, 679, 746R

[8] Schmid, H. M., Bazzon, A., Milli, J., *et al.* 2017, A&A, 602, A53

[9] Solf, J., & Ulrich, H. 1985, A&A, 148, 274